

Complementation between mouse Mfn1 and Mfn2 protects mitochondrial fusion defects caused by CMT2A disease mutations

Scott A. Detmer and David C. Chan

Division of Biology, California Institute of Technology, Pasadena, CA 91125

Mfn2, an oligomeric mitochondrial protein important for mitochondrial fusion, is mutated in Charcot-Marie-Tooth disease (CMT) type 2A, a peripheral neuropathy characterized by axonal degeneration. In addition to homooligomeric complexes, Mfn2 also associates with Mfn1, but the functional significance of such heterooligomeric complexes is unknown. Also unknown is why Mfn2 mutations in CMT2A lead to cell type-specific defects given the widespread expression of Mfn2. In this study, we show that homooligomeric complexes formed by many Mfn2 disease mutants are nonfunctional for mitochondrial fusion.

However, wild-type Mfn1 complements mutant Mfn2 through the formation of heterooligomeric complexes, including complexes that form in trans between mitochondria. Wild-type Mfn2 cannot complement the disease alleles. Our results highlight the functional importance of Mfn1–Mfn2 heterooligomeric complexes and the close interplay between the two mitofusins in the control of mitochondrial fusion. Furthermore, they suggest that tissues with low Mfn1 expression are vulnerable in CMT2A and that methods to increase Mfn1 expression in the peripheral nervous system would benefit CMT2A patients.

Introduction

Mitofusins are mitochondrial outer membrane GTPases required for mitochondrial fusion (Chan, 2006). Although yeast have one mitofusin, Fzo1 (Okamoto and Shaw, 2005), mammals contain two mitofusins, Mfn1 and Mfn2 (Santel and Fuller, 2001; Rojo et al., 2002; Chen et al., 2003). In the absence of either Mfn1 or Mfn2, cells have greatly reduced levels of mitochondrial fusion, and the imbalance of fusion and fission events leads to mitochondrial fragmentation (Chen et al., 2003). In the absence of both Mfn1 and Mfn2, no mitochondrial fusion can occur, leading to severe mitochondrial and cellular dysfunction (Chen et al., 2005). Moreover, mitochondrial dynamics play an important role in apoptosis (Youle and Karbowski, 2005), and maintenance of mitochondrial fusion has been linked to protection against apoptosis (Olichon et al., 2003; Sugioka et al., 2004; Neuspiel et al., 2005).

Mutations in Mfn2 cause Charcot-Marie-Tooth disease (CMT) type 2A, an autosomal dominant peripheral neuropathy (Zuchner et al., 2004). Most types of CMT disease involve

Schwann cell dysfunction, resulting in the demyelination of peripheral nerves. However, CMT2A is an axonal form in which the axons of the longest sensory and motor nerves are selectively affected (Zuchner and Vance, 2005). There is currently no effective treatment for this disease. Interestingly, another neurodegenerative disease, dominant optic atrophy, is caused by mutations in OPA1 (Alexander et al., 2000; Delettre et al., 2000), a mitochondrial intermembrane space protein that is also necessary for mitochondrial fusion. The sensitivity of neurons to mutations in Mfn2 and OPA1 suggests that such cells are particularly dependent on mitochondrial dynamics, which likely impacts the recruitment of mitochondria to extended neuronal processes (Chen and Chan, 2006). Indeed, the disruption of mitochondrial dynamics has been experimentally linked to neuronal dysfunction (Stowers et al., 2002; Li et al., 2004; Guo et al., 2005; Verstreken et al., 2005).

Several issues regarding mitofusin function and its relation to neurodegenerative disease remain poorly understood. First, it is unclear to what extent there is functional interplay between Mfn1 and Mfn2 during mitochondrial fusion. In experiments with Mfn1- or Mfn2-null cells, either mitofusin can functionally replace the other, indicating functional redundancy (Chen et al., 2003, 2005). However, some studies

Correspondence to David C. Chan: dchan@caltech.edu

Abbreviations used in this paper: CMT, Charcot-Marie-Tooth disease; ES, embryonic stem; MEF, mouse embryonic fibroblast; PEG, polyethylene glycol.

The online version of this article contains supplemental material.

suggest distinct pathways or mechanisms for Mfn1 versus Mfn2 (Cipolat et al., 2004; Ishihara et al., 2004). OPA1 action has been reported to depend on Mfn1 but not Mfn2 (Cipolat et al., 2004). An in vitro study indicates that overexpressed Mfn1 is more effective than Mfn2 in tethering mitochondria, an effect that is correlated with a higher rate of GTP hydrolysis for Mfn1 (Ishihara et al., 2004). Second, Mfn1 and Mfn2 have been shown to physically associate with each other (Chen et al., 2003; Eura et al., 2003), but the functional significance of such heterooligomeric complexes is poorly understood. Finally, it is unknown why Mfn2 mutations in CMT2A cause such highly cell type-specific defects. Patients with CMT2A show deficits in the longest sensory and motor peripheral nerves, with a subset showing additional degeneration in the optic nerve (Zuchner and Vance, 2005). The length-dependent degeneration of peripheral nerves likely reflects an inherent challenge of neurons to supply functional mitochondria to the nerve terminals, but it remains unclear why primarily the peripheral and optic nerves are affected.

In this study, we have analyzed Mfn2 disease alleles that cause CMT2A. We find that most of these mutants are not functional for fusion when allowed to form only homotypic complexes. However, these Mfn2 mutants can be complemented

through the formation of heterotypic complexes with wild-type Mfn1. These results emphasize the close interplay between Mfn1 and Mfn2 in the mitochondrial fusion reaction, demonstrate the functional importance of Mfn1–Mfn2 heterooligomeric complexes, and provide insights into the pathogenesis of Mfn2-dependent neuropathy.

Results

Many Mfn2 CMT2A alleles fail to rescue mitochondrial morphology in double Mfn-null cells

We have previously generated mouse embryonic fibroblast (MEF) cell lines with null mutations in both Mfn1 and Mfn2 (double Mfn-null cells; Koshiba et al., 2004; Chen et al., 2005). These cell lines enable straightforward structure-function analysis of mouse mitofusins. Human and mouse Mfn2 are 95% identical, and all of the residues that were found mutated in the original CMT2A study (Zuchner et al., 2004) are conserved in mouse Mfn2. In the present study, we introduced nine of the originally reported point mutations into mouse Mfn2; these include mutations occurring immediately before the GTPase domain (V69F and L76P), within the GTPase domain (R94Q, R94W,

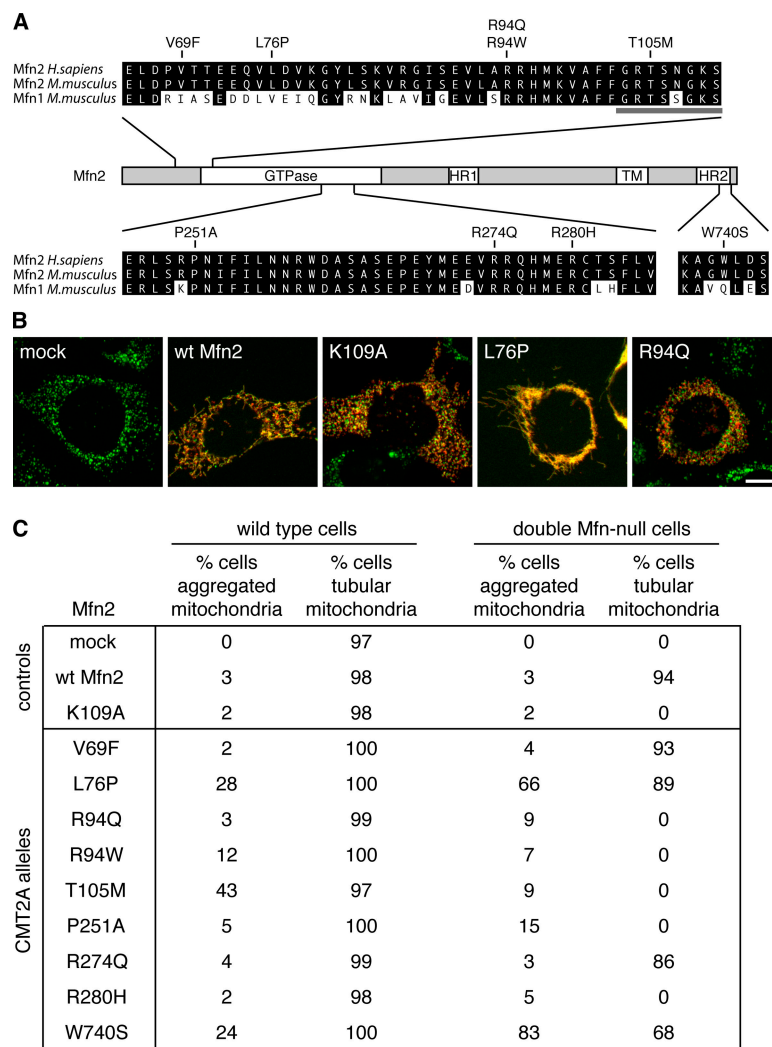


Figure 1. Functional analysis of Mfn2 CMT2A alleles.

(A) Domain structure of Mfn2 with the GTPase, hydrophobic heptad repeat (HR), and transmembrane regions (TM) indicated. A sequence alignment of human Mfn2 with mouse Mfn2 and Mfn1 is shown for the regions surrounding CMT2A point mutations. Note that the residues mutated in CMT2A disease are conserved between human and mouse Mfn2. The horizontal gray bar indicates the GTPase G1 motif. (B) Representative images of double Mfn-null cells expressing myc-tagged Mfn2 at a low multiplicity of infection. Mitochondria are visualized by matrix-targeted EGFP (green), and Mfn2-expressing cells are identified by immunofluorescence against the myc epitope (red). Note mitochondrial aggregation induced by the CMT2A allele L76P. Bar, 10 μ m. (C) Summary of mitochondrial profiles when Mfn2 CMT2A alleles are expressed in wild-type MEFs (left two columns) and double Mfn-null MEFs (right two columns). In each case, infected cells were scored for mitochondrial morphology, and the three categories of tubular mitochondria (Fig. S1, A and B; available at <http://www.jcb.org/cgi/content/full/jcb.200611080/DC1>) were added to yield the percentage of cells with tubular mitochondria. Mitochondrial aggregation was independently scored. More than 150 cells were scored for each experiment. As additional reference points, using the same scoring criteria, we find that 0% of Mfn1-null cells and 10% of Mfn2-null cells have tubular mitochondria (see controls in Fig. 6, C and D).

T105M, P251A, R274Q, and R280H), and in a C-terminal heptad repeat region (W740S; Fig. 1 A). By expressing these disease alleles in wild-type and double Mfn-null MEFs, we could assess their subcellular localization, effects on mitochondrial morphology, and ability to mediate mitochondrial fusion.

Mock-infected wild-type MEFs have a range of mitochondrial profiles, but the vast majority of cells show considerable amounts of tubular mitochondria (Fig. 1 C and Fig. S1 A, available at <http://www.jcb.org/cgi/content/full/jcb.200611080/DC1>). The expression of wild-type Mfn2 or the GTPase mutant Mfn2^{K109A} by retroviral transduction did not affect mitochondrial morphology. We found that all of the CMT2A mutants properly localized to mitochondria as determined by immunofluorescence. However, seven of the nine CMT2A alleles (all except Mfn2^{V69F} and Mfn2^{R274Q}) caused substantial mitochondrial aggregation when cells were infected at a high multiplicity of infection (Fig. S2). At low infection rates, most infected cells have only one proviral copy and express about fourfold Mfn2 compared with endogenous Mfn2 in wild-type cells (Fig. S3). Under these conditions, only Mfn2^{L76P}, Mfn2^{T105M}, and Mfn2^{W740S} caused high levels of mitochondrial aggregation (Fig. 1 C). In contrast, such mitochondrial aggregation was not found in cells expressing wild-type Mfn2 and was found only in a few cells expressing Mfn2^{K109A}. This mitochondrial aggregation phenotype may reflect the aberration of Mfn2 function by CMT2A mutations; however, the effect is clearly dosage dependent and is not observed at physiological expression levels (see Fig. 4). Therefore, its relevance to CMT2A disease remains to be determined.

To evaluate the Mfn2 CMT2A alleles for mitochondrial fusion activity, we expressed them in double Mfn-null cells. Cells lacking mitofusins are fully deficient for mitochondrial fusion and show completely fragmented mitochondrial morphology (Chen et al., 2005). The expression of wild-type Mfn2 restored mitochondrial fusion, resulting in tubular mitochondrial morphology (Fig. 1, B and C; and Fig. S1 B). In contrast, the GTPase mutant Mfn2^{K109A} behaved as a complete loss of

function allele, showing no ability to restore mitochondrial tubules. The CMT2A mutants Mfn2^{R94Q}, Mfn2^{R94W}, Mfn2^{T105M}, Mfn2^{P251A}, and Mfn2^{R280H} are similarly unable to promote mitochondrial tubules in double Mfn-null cells. In contrast, cells expressing Mfn2^{V69F}, Mfn2^{L76P}, Mfn2^{R274Q}, or Mfn2^{W740S} showed a considerable restoration of mitochondrial tubules. Therefore, more than half of the CMT2A mutants are nonfunctional.

Nonrescuing CMT2A alleles lack mitochondrial fusion activity

To definitively evaluate the fusion activity of CMT2A alleles, we tested them in a polyethylene glycol (PEG) mitochondrial fusion assay. In this assay, double Mfn-null cells containing either mitochondrially targeted EGFP or mito-DsRed were each infected with retrovirus expressing a CMT2A allele. Hybrids between the two cell lines were scored for mitochondrial fusion. Cell hybrids that formed between double Mfn-null cells or cells expressing Mfn2^{K109A} never showed mitochondrial fusion (Fig. 2). In contrast, the expression of wild-type Mfn2 resulted in extensive mitochondrial fusion: 75% of the cell hybrids exhibited a complete overlay of EGFP and DsRed (scored as full fusion) or a nearly complete overlay with some singly labeled mitochondria remaining (scored as extensive fusion). 20% of these hybrids had no colabeled mitochondria (scored as no fusion) and invariably had fragmented mitochondria. These hybrids likely arose from uninfected cells. When clonal infected cell lines were used (Koshiba et al., 2004), all cell hybrids showed extensive mitochondrial fusion.

We found excellent agreement between the ability of a CMT2A allele to restore mitochondrial tubules to double Mfn-null cells and their fusion activity in the PEG assay. The Mfn2 CMT2A alleles Mfn2^{V69F}, Mfn2^{L76P}, Mfn2^{R274Q}, and Mfn2^{W740S} induced fluorophore mixing as efficiently as wild-type Mfn2, indicating that they are highly functional. In contrast, mutants Mfn2^{R94Q}, Mfn2^{R94W}, Mfn2^{T105M}, Mfn2^{P251A}, and Mfn2^{R280H} were all completely deficient for mitochondrial fusion. Interestingly, the five nonfunctional alleles are all in positions that are

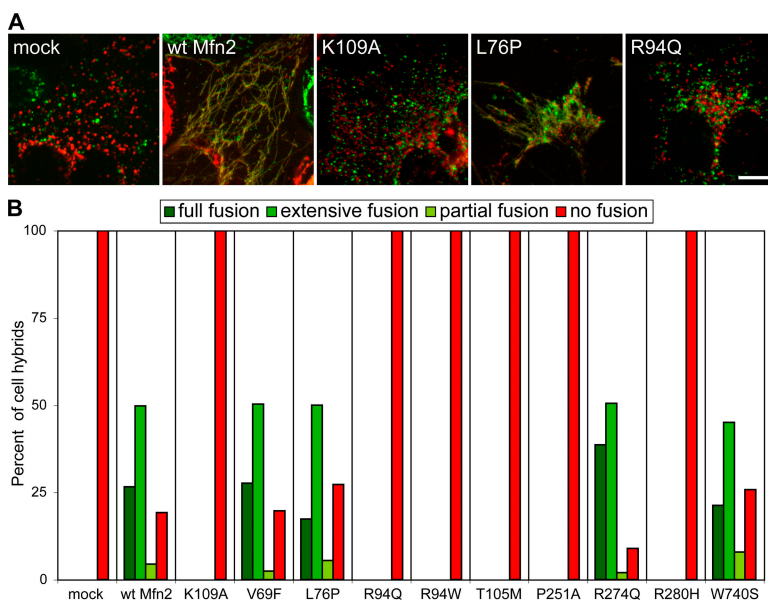


Figure 2. Lack of mitochondrial fusion activity in many CMT2A alleles. Double Mfn-null cells expressing either mito-DsRed or mito-EGFP were infected with the same Mfn2 construct. The PEG fusion assay was used to evaluate mitochondrial fusion activity in cell hybrids formed from such cells. (A) Representative merged images of cell hybrids. No fusion is detected with mock-, Mfn2^{K109A}-, or Mfn2^{R94Q}-infected cells. Extensive fusion is observed with wild-type Mfn2 and Mfn2^{L76P}. Bar, 10 μ m. (B) Quantitation of mitochondrial fusion in cell hybrids. More than 200 cell hybrids were scored per experiment.

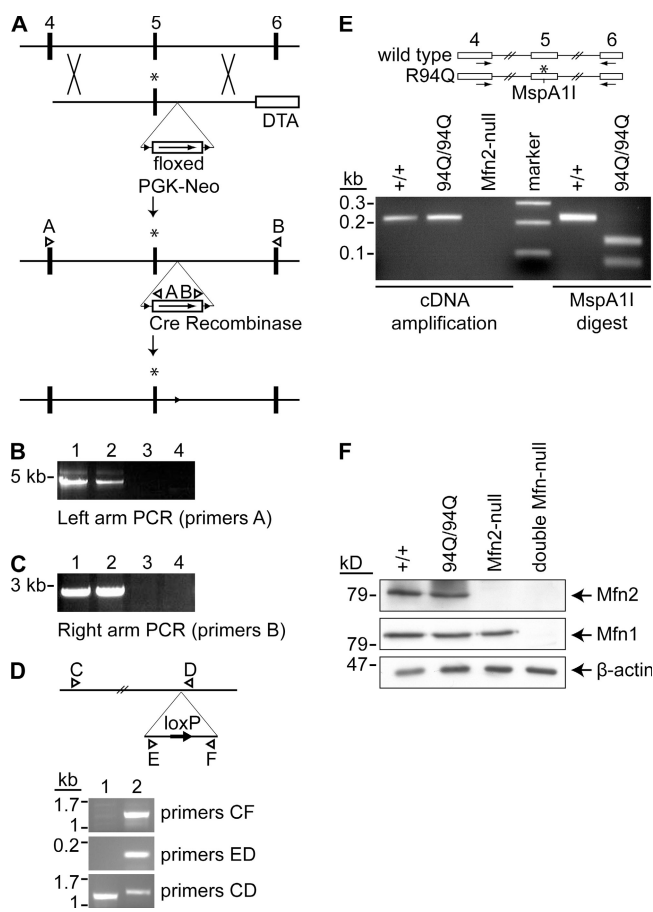


Figure 3. Construction of MEFs containing homozygous *Mfn2*^{R94Q} knockin mutations. (A) Schematic of *Mfn2* targeting construct and strategy. A portion of the *Mfn2* genomic locus containing exons 4–6 is shown on top based on Ensembl transcript ID ENSMUST0000030884 (www.ensembl.org). The knockin targeting vector below contains the R94Q mutation (*) placed in exon 5 as well as a floxed neomycin cassette for positive selection and a diphtheria toxin cassette (DTA) for negative selection. Homologous recombination in ES cells leads to the configuration in the third line, which can be detected by PCR using the A and B pairs of primers (triangles), as shown in B and C. Mice were generated with the targeted ES cells, and Cre recombination in vivo was used to excise the neomycin cassette, leading to the bottom configuration containing the R94Q mutation and *loxP* scar (arrowhead). (B) PCR screen of ES cells using primer set A for detection of the correct targeting of the left arm. Four ES cell clones are shown; the first two clones are positive. Because the 5' primer is outside the targeting construct, only correctly targeted clones will yield the desired PCR product. (C) PCR screen of ES cells using primer set B for detection of the correct targeting of the right arm. The same two ES cell clones are positive. Note that the 3' primer is outside the targeting construct. (D) PCR screen of *Mfn2* genomic structure after in vivo Cre-mediated excision of the PGK-neomycin cassette. Excision leaves behind a 140-bp *loxP* scar as diagrammed. Three sets of PCR reactions were used to confirm the presence of the *loxP* scar in *Mfn2*^{R94Q} homozygous MEFs (lane 2) but not wild-type MEFs (lane 1). (E) Genotype assay for *Mfn2* transcripts. The schematic on top shows the genomic *Mfn2* locus containing exons 4–6. Exon 5 encodes residue 94. A cDNA fragment was amplified using the indicated primers in exons 4 and 6. cDNA amplification and restriction digestion was performed on first-strand cDNA from wild-type (+/+), *Mfn2*^{R94Q}-*Mfn2*^{R94Q}, and *Mfn2*-null cells. In the *Mfn2*^{R94Q} cDNA, the engineered R94Q mutation (*) introduces a *MspA11* site, resulting in cleavage of the 233-bp PCR product into 146- and 87-bp fragments. (F) Expression of Mfn1 and the *Mfn2*^{R94Q} allele at endogenous levels. Postnuclear whole cell lysates from the indicated MEFs were separated by SDS-PAGE and immunoblotted with an anti-Mfn2 (top) or Mfn1 antibody (middle). β -actin was used as a loading control (bottom).

conserved between Mfn1 and Mfn2. Three of the four functional alleles are in nonconserved positions.

Endogenous *Mfn1* functionally complements the CMT2A mutant *Mfn2*^{R94Q} to induce mitochondrial fusion

Our PEG fusion assays showed that *Mfn2*^{R94Q}, along with four other CMT2A alleles, has no mitochondrial fusion activity in double *Mfn*-null cells. This allele is particularly interesting because position 94 is the most commonly mutated residue found in CMT2A. Multiple clinical studies have found familial or de novo mutations of residue 94 to either Q or W (Zuchner et al., 2004, 2006; Kijima et al., 2005; Chung et al., 2006; Verhoeven et al., 2006). To definitively study the in vivo properties of this allele, we used homologous recombination to place the R94Q mutation into the endogenous mouse *Mfn2* locus in embryonic stem (ES) cells (Fig. 3, A–D). For positive selection, the targeting construct contained a neomycin expression cassette flanked by *loxP* sites. After the generation of mice containing the knockin allele, Cre-mediated recombination was used to excise the neomycin cassette in vivo, resulting in an *MFN2* locus containing the R94Q mutation and a short *loxP* scar located in the adjacent intron (Fig. 3, A and D). We mated mice heterozygous for the *Mfn2*^{R94Q} allele, and homozygous embryos were used to derive *Mfn2*^{R94Q} homozygous MEF cell lines.

Our molecular analyses indicate that these cell lines express no wild-type *Mfn2* while expressing endogenous levels of *Mfn2*^{R94Q} (Fig. 3, E and F). To confirm the expression of *Mfn2*^{R94Q} in these cell lines, we used RT-PCR to analyze *Mfn2* RNA transcripts. We amplified exon 5 (which encodes residue 94) and the adjoining sequences of *Mfn2* cDNA by PCR. The presence of the R94Q mutation within the amplified cDNA fragment was diagnosed by digestion with the restriction enzyme *MspA11*, which cuts uniquely at a site introduced by the R94Q mutation. As expected, the cDNA fragment was amplified from cDNA of wild-type and *Mfn2*^{R94Q} homozygous cells but not *Mfn2*-null cells (Fig. 3 E). The cDNA from wild-type cells is completely resistant to *MspA11* digestion, whereas the cDNA from *Mfn2*^{R94Q} homozygous cells was completely digested by *MspA11*, demonstrating that all *Mfn2* transcripts contain the R94Q mutation. Having confirmed mRNA expression of the mutant allele, we next confirmed protein expression. Immunoblot analysis indicated that endogenous levels of Mfn1 and Mfn2 are present in wild-type and *Mfn2*^{R94Q} homozygous cell lines (Fig. 3 F).

Given that *Mfn2*^{R94Q} has no fusion activity in double *Mfn*-null cells (Figs. 1 and 2), we expected *Mfn2*^{R94Q} homozygous cells to have fragmented mitochondria similar to those found in *Mfn2*-null cells (Chen et al., 2003, 2005). Surprisingly, the scoring of mitochondrial profiles indicated that most *Mfn2*^{R94Q} homozygous cells have predominantly tubular mitochondria; this is in striking contrast to *Mfn2*-null cells, which have extensive mitochondrial fragmentation (Fig. 4, A and B). In addition, we did not find any mitochondrial aggregation in the *Mfn2*^{R94Q} homozygous cell line.

Therefore, although *Mfn2*^{R94Q} behaves as a null allele when expressed in double *Mfn*-null cells, it is clearly highly functional in our homozygous knockin cells. In evaluating these results, it is important to consider the total complement

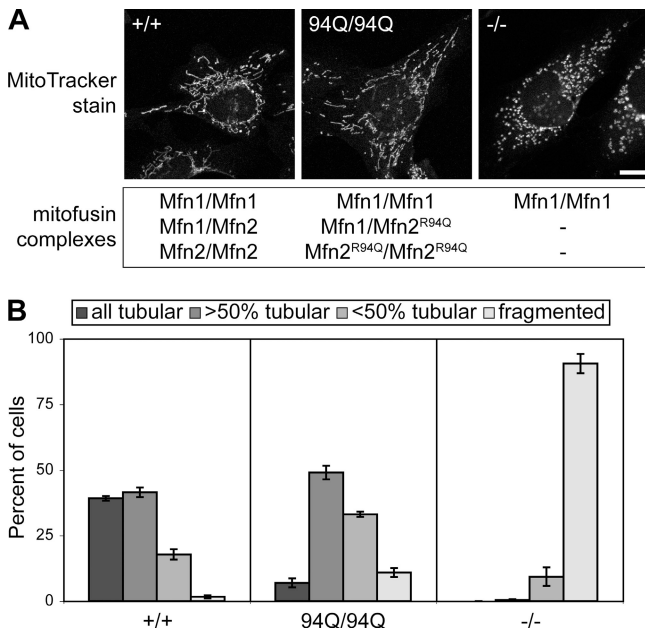


Figure 4. **Tubular mitochondria in Mfn2^{R94Q}-Mfn2^{R94Q} cells.** (A) Representative images of mitochondrial morphology in wild-type (+/+), Mfn2^{R94Q}-Mfn2^{R94Q}, and Mfn2-null (-/-) cells. Mitochondria were visualized by MitoTracker red staining. Below each cell, the potential mitofusin oligomers are listed. Bar, 10 μ m. (B) Quantitation of mitochondrial morphology. For each cell line, 100 cells were scored in three independent experiments. Error bars indicate SD.

of mitofusins in each cellular context because Mfn1 and Mfn2 can form both homooligomeric (Mfn1-Mfn1 or Mfn2-Mfn2) and heterooligomeric (Mfn1-Mfn2) complexes (Chen et al., 2003; Eura et al., 2003). When Mfn2^{R94Q} is expressed in double Mfn-null cells, only Mfn2^{R94Q}-Mfn2^{R94Q} homooligomeric complexes can be formed, and such complexes are clearly inactive for mitochondrial fusion. In Mfn2^{R94Q} homozygous knockin cells, endogenous Mfn1 is still present (Fig. 3 F). Therefore, three possible complexes can be formed: Mfn1-Mfn1, Mfn1-Mfn2^{R94Q}, and Mfn2^{R94Q}-Mfn2^{R94Q} (Fig. 4 A). The phenotype of Mfn2-null cells (which contain only Mfn1-Mfn1 homooligomeric complexes) indicates that endogenous levels of Mfn1-Mfn1 complexes alone are not sufficient to promote tubular mitochondria. Given that Mfn2^{R94Q}-Mfn2^{R94Q} complexes are nonfunctional (Fig. 2), these results strongly suggest that Mfn2^{R94Q} can cooperate with Mfn1 to form Mfn1-Mfn2^{R94Q} complexes capable of promoting fusion.

Mfn2 CMT2A mutants physically associate with wild-type Mfn1 and Mfn2

If this model of complementation is correct, Mfn2^{R94Q} should be able to physically associate with wild-type Mfn1. We tested whether the Mfn2 CMT2A mutants could coimmunoprecipitate with wild-type Mfn1 and Mfn2. In MEFs, all of the Mfn2 CMT2A mutants associated with Mfn1 at normal levels with the exception of Mfn2^{T105M}, which showed lower levels (Fig. 5 A). Similarly, the Mfn2 CMT2A mutants associated with Mfn2, although at slightly reduced levels compared with wild-type Mfn2. Again, Mfn2^{T105M} had low binding. It should be noted that when analogous immunoprecipitation experiments were performed in transfected 293T cells, the reduction in Mfn2^{T105M} binding was subtle (unpublished data). Therefore, although Mfn2^{T105M} has reduced binding to wild-type Mfn1 and Mfn2, this defect is not observed at high expression levels. The engineered GTPase mutant Mfn2^{K109A}, which interacted strongly with Mfn1, interacted poorly with Mfn2. These results suggest that the mutant Mfn2 molecules can interact with wild-type Mfn1 and Mfn2 and can potentially participate in or modify the fusion reaction.

Mfn1 but not Mfn2 complements CMT2A alleles to induce mitochondrial fusion

To learn more about the complementation of Mfn1 and Mfn2^{R94Q} and whether this is a unique property of the Mfn2^{R94Q} allele, we tested all of the nonfunctional Mfn2 CMT2A alleles for complementation with wild-type Mfn1 and Mfn2. We expressed alleles Mfn2^{R94Q}, Mfn2^{R94W}, Mfn2^{T105M}, Mfn2^{P251A}, and Mfn2^{R280H} in either Mfn2- or Mfn1-null cells and scored mitochondrial profiles. Most Mfn2-null cells have fragmented mitochondrial morphology, with only ~13% of the cells having short mitochondrial tubules. The expression of wild-type Mfn2 in these cells restores normal tubular mitochondrial morphology (Fig. 6, A and C). Remarkably, the expression of each of the five CMT2A alleles into Mfn2-null cells resulted in extensive mitochondrial tubulation. The GTPase mutant Mfn2^{K109A} was also able to induce mitochondrial tubulation, although its effect was considerably weaker than that of the CMT2A alleles. Because Mfn2-null cells contain Mfn1, the expression of CMT2A alleles in Mfn2-null cells results in the formation of three possible complexes: Mfn1-Mfn1, Mfn1-Mfn2^{CMT2A}, and Mfn2^{CMT2A}-Mfn2^{CMT2A} (Fig. 6 A). These results strongly support and generalize our interpretation of the Mfn2^{R94Q} homozygous

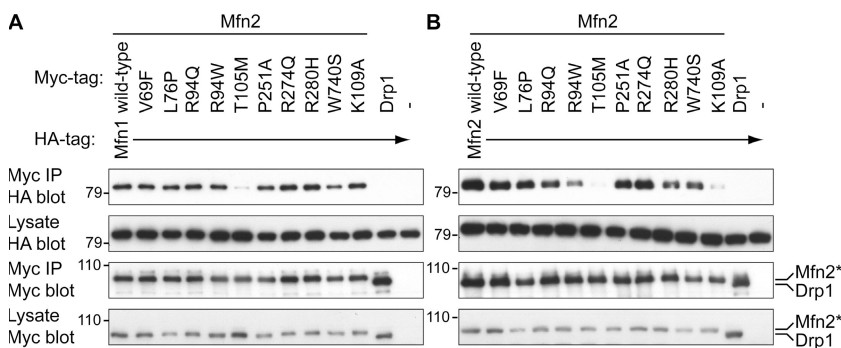


Figure 5. **Physical association of mutant Mfn2 with wild-type Mfn1 and Mfn2.** (A) Myc-tagged Mfn2 mutants were expressed in double Mfn-null cell lines stably expressing HA-tagged Mfn1. Anti-myc immunoprecipitates (myc IP) and postnuclear lysates (lysate) were analyzed by Western blotting with anti-myc and anti-HA antibodies. Mock (-) or Drp1-myc-infected cells were used as negative controls. The relative load of the immunoprecipitates was 14 times that of the lysates. (B) Same as in A except performed in double Mfn-null cell lines stably expressing HA-tagged Mfn2. Positions of the Mfn2-myc and Drp1-myc bands and positions of molecular mass markers (given in kilodaltons) are indicated.

knockin cell line: Mfn2 disease alleles can cooperate with Mfn1 to promote fusion activity. This activity is likely mediated by Mfn1–Mfn2^{CMT2A} heterooligomers. Because even mutant Mfn2^{K109A} shows a low level of complementation with Mfn1, Mfn2 need not have GTPase activity to cooperate with Mfn1.

In contrast, the expression of mutants Mfn2^{R94Q}, Mfn2^{R94W}, Mfn2^{T105M}, Mfn2^{P251A}, and Mfn2^{R280H} in Mfn1-null cells did not induce tubulation (Fig. 6, B and D). Mfn1-null cells expressing these alleles had extensively fragmented mitochondria. In this experiment, only Mfn2 complexes can be formed: Mfn2–Mfn2, Mfn2^{CMT2A}–Mfn2^{CMT2A}, and Mfn2–Mfn2^{CMT2A} (Fig. 6 B). Therefore, in contrast to Mfn1–Mfn2^{CMT2A} complexes, Mfn2–Mfn2^{CMT2A} complexes do not appear to be competent for fusion.

Complementation between mutant Mfn2 and Mfn1 in trans

The aforementioned experiments demonstrate that Mfn1 can complement Mfn2 CMT2A alleles. By the nature of the experiment, it is impossible to know whether the complementation is occurring on the same mitochondria (in cis), between adjacent mitochondria (in trans), or both. To test whether the nonfunctional Mfn2 mutants can support fusion with wild-type mitochondria in trans, we returned to the PEG cell hybrid assay for mitochondrial fusion. In this assay, mitochondria from double

Mfn-null cells cannot fuse with mitochondria from wild-type cells, indicating a requirement for mitofusins on adjacent mitochondria (Koshiba et al., 2004; Chen et al., 2005). We expressed Mfn2 alleles in double Mfn-null cells and assessed mitochondrial fusion in cell hybrids with wild-type cells. In this experimental scheme, Mfn2^{CMT2A}–Mfn2^{CMT2A} complexes present on one set of mitochondria are tested for fusion with mitochondria containing a full complement of wild-type mitofusin complexes (Mfn1–Mfn1, Mfn2–Mfn2, and Mfn1–Mfn2 complexes). As expected, when double Mfn-null cells expressing wild-type Mfn2 were fused with wild-type cells, we found extensive colabeling of mitochondria (Fig. 7 B). Moreover, the Mfn2 CMT2A alleles Mfn2^{R94Q}, Mfn2^{R94W}, Mfn2^{P251A}, and Mfn2^{R280H} induce readily detectable but moderate levels of fusion that are lower than those of wild-type Mfn2 but are much more than those of Mfn2^{K109A} (Fig. 7, A and B). However, the Mfn2^{T105M} allele allows essentially no mitochondrial fusion. These results indicate that most Mfn2 CMT2A mutants can function in trans with wild-type mitofusin complexes.

To determine whether this complementation is caused by interactions with wild-type Mfn1–Mfn1 or Mfn2–Mfn2 complexes, we next tested the Mfn2 CMT2A alleles in mitochondrial fusion assays with Mfn2-null and Mfn1-null cells. Mfn2 mutants Mfn2^{R94Q}, Mfn2^{R94W}, Mfn2^{P251A}, and Mfn2^{R280H}

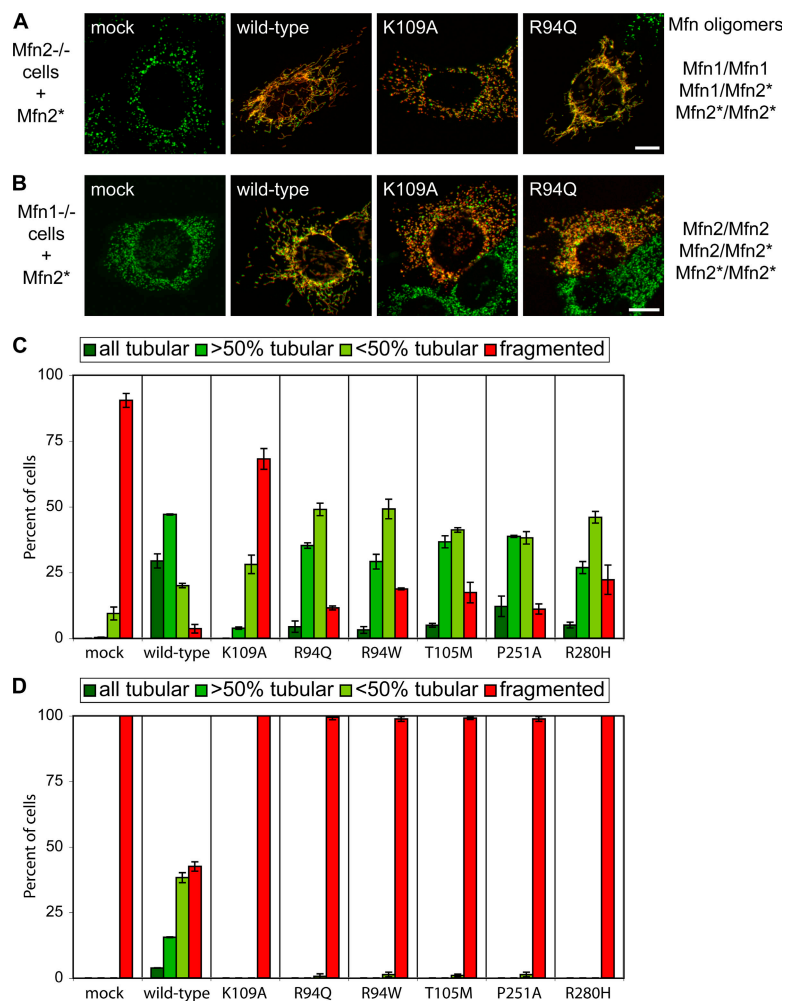


Figure 6. Mfn1 but not Mfn2 complements Mfn2 CMT2A alleles. (A and B) Representative images of mitochondrial morphology in Mfn2-null (A) or Mfn1-null MEFs (B) expressing myc-tagged Mfn2 alleles. Mitochondria are visualized by mitochondrially targeted EGFP (green), and the infected cells are detected by anti-myc immunofluorescence (red). Note that Mfn2^{R94Q} promotes tubulation in Mfn2-null but not Mfn1-null MEFs. The potential mitofusin complexes in each experiment are listed on the right, with the CMT2A mutant molecule indicated by Mfn2*. Bars, 10 μ m. (C and D) Quantitation of mitochondrial morphology in Mfn2- (C) and Mfn1-null MEFs (D) expressing Mfn2 CMT2A alleles. In Mfn1-null MEFs, very short mitochondrial tubules were scored as fragmented. 150 cells were scored in two independent experiments. Error bars indicate SD.

promoted moderate levels of mitochondrial fusion in cell hybrids with Mfn2-null cells (Fig. 7, A and C). In contrast, the same mutants induced no mitochondrial fusion in hybrids with Mfn1-null cells (Fig. 7, A and D). These results demonstrate that most Mfn2^{CMT2A} alleles can promote fusion when exposed to membranes containing Mfn1 but not Mfn2. As expected from its failure to promote fusion with wild-type mitochondria, Mfn2^{T105M} showed no fusion activity with either the Mfn2- or Mfn1-null cells.

Discussion

The Mfn1-Mfn2 heterooligomeric complex is an important regulator of mitochondrial dynamics

Previous immunoprecipitation studies indicated that Mfn1 and Mfn2 form heterooligomeric complexes (Chen et al., 2003; Eura et al., 2003). However, most functional studies have focused on Mfn1 or Mfn2 in isolation, and, therefore, we have little information on the functional importance of the heterooligomeric complex. The only direct demonstration that this complex is functional comes from the observation that cell hybrids between Mfn1- and Mfn2-null cells show low levels of mitochondrial fusion, suggesting that Mfn1-Mfn2 heterotypic complexes formed in trans have fusion activities that are roughly comparable with homooligomeric Mfn1 or Mfn2 complexes alone (Chen et al., 2005). Our current study of Mfn2 disease alleles reveals an intimate interplay between Mfn1 and Mfn2 in mediating mitochondrial fusion. A subset of Mfn2 disease alleles lack mitochondrial fusion activity in isolation but show substantial fusion activity in the presence of Mfn1. In addition, PEG fusion assays (Fig. 7) indicate that this cooperation between Mfn1 and mutant Mfn2 at least partially occurs through interactions in trans. Such close physical and functional interactions between Mfn1 and Mfn2 support the view that they have similar biochemical functions during mitochondrial membrane fusion. These results highlight the importance of heterooligomeric Mfn1-Mfn2 complexes in the control of mitochondrial dynamics.

Our study greatly extends a different type of complementation demonstrated in the yeast mitofusin Fzo1p. Fzo1p demonstrates strong complementation between specific pairs of null alleles, resulting in the restoration of mitochondrial tubules (Griffin and Chan, 2006). For example, an *fzo1* mutant containing a GTPase mutation can cooperate with an *fzo1* mutant containing a heptad repeat mutation to promote mitochondrial fusion. Such complementation reflects the oligomeric nature of mitofusin complexes and indicates that each subunit of the oligomer need not be fully functional to provide function to the complex. However, this previous study (Griffin and Chan, 2006) was limited to Fzo1 homooligomeric complexes, unlike the heterooligomeric complexes studied here. Indeed, we have not been able to demonstrate a similar type of complementation in Mfn1 or Mfn2 homooligomeric complexes (unpublished data).

Functional heterogeneity of CMT2A alleles

Our results reveal some functional heterogeneity in Mfn2 mutants that underlie CMT2A disease. The Mfn2^{T105M} allele

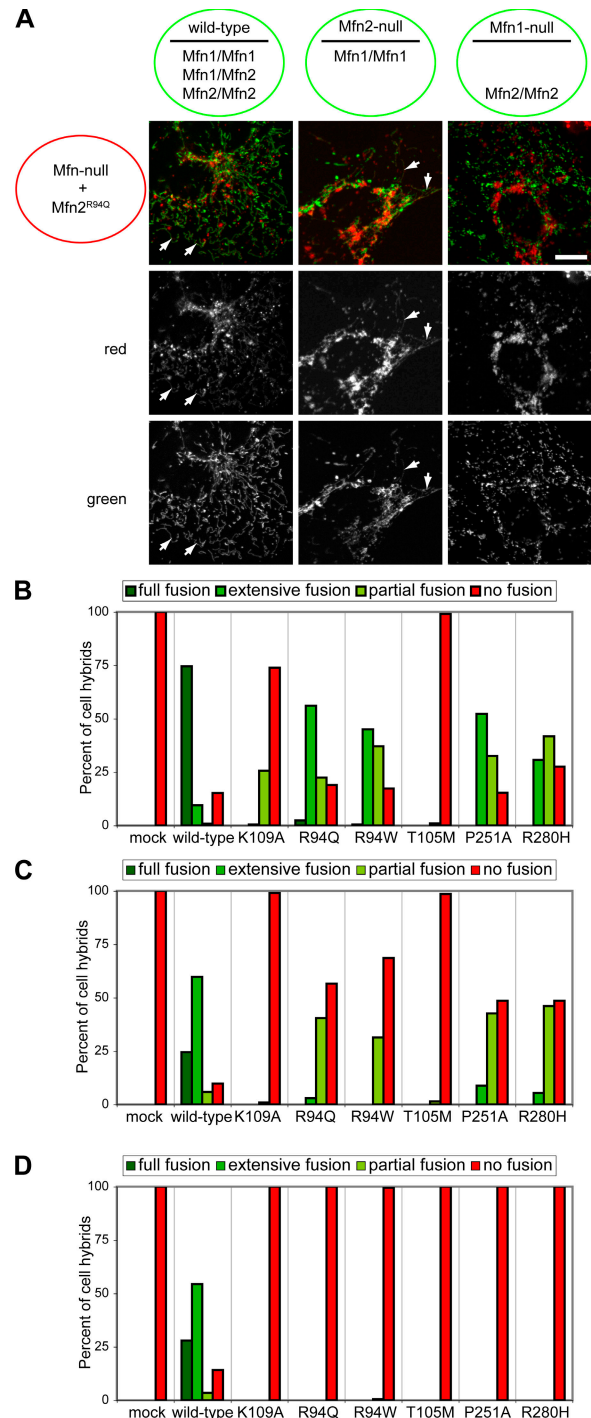


Figure 7. Mfn1 complements Mfn2 CMT2A mutants in trans. (A) Double Mfn-null MEFs expressing mitochondrial DsRed and Mfn2R94Q were fused to wild-type cells (left), Mfn2-null cells (middle), or Mfn1-null cells (right). As indicated by the green circles, the latter three cell lines expressed mitochondrial EGFP. For each cell line, all potential mitofusin oligomers are listed under the horizontal line. Colabeled mitochondrial tubules (indicated with arrows) are clearly observed in cell hybrids with wild-type and Mfn2-null cells but not with Mfn1-null cells. Bar, 10 μ m. (B–D) Double Mfn-null cells expressing the indicated Mfn2 mutant were assayed for mitochondrial fusion in cell hybrids with wild-type cells (B), Mfn2-null cells (C), and Mfn1-null cells (D). For each PEG fusion assay, at least 200 cell hybrids were scored.

behaved somewhat differently from the other nonfunctional alleles. Mfn2^{T105M}, like the other nonfunctional alleles, could be complemented by wild-type Mfn1. However, it showed reduced physical interactions with Mfn1 and did not show complementation with Mfn1 in trans. Presumably, Mfn2^{T105M} can be complemented by Mfn1 in cis but not in trans.

Over half of the CMT2A alleles are nonfunctional in double Mfn-null cells, but the rest show substantial fusion activity. More sensitive assays will be necessary to understand how the functional alleles affect mitochondrial dynamics. Some of the functional alleles caused severe mitochondrial aggregation when overexpressed. Future studies will determine the physiological significance of this phenotype.

Implications for pathogenesis and treatment of CMT2A

Our results have important implications for understanding the pathogenesis of CMT2A, especially because four of the five nonfunctional mutant alleles described in this study (Mfn2^{R94Q}, Mfn2^{R94W}, Mfn2^{T105M}, and Mfn2^{R280H}) are among the most commonly identified Mfn2 mutations (Zuchner et al., 2004, 2006; Kijima et al., 2005; Lawson et al., 2005; Chung et al., 2006; Verhoeven et al., 2006). In contrast to the broad expression pattern of Mfn2, one of the remarkable features of CMT2A disease is its apparent cell type specificity. In most patients, the clinical features are restricted to the motor and sensory neurons of the peripheral nervous system. In a subset of patients (designated as hereditary motor and sensory neuropathy type VI), the optic nerve is additionally affected (Zuchner et al., 2006). A recent study has suggested possible involvement of the central nervous system (Chung et al., 2006). This clinical picture suggests that most cells in CMT2A patients likely have only mild perturbations in mitochondrial dynamics. Moreover, in a typical patient, only the longest peripheral sensory and motor neurons are affected. This length dependence suggests that even in the peripheral nervous system, the defects in mitochondrial dynamics are not catastrophic because only the neurons with the highest demands for precise control of mitochondrial fusion are damaged.

Our studies of the Mfn2^{R94Q} knockin mice are ongoing, but initial observations support the conclusion that CMT2A disease results from a mild perturbation in mitochondrial dynamics. Thus far, we have not observed a neurological phenotype in the heterozygous knockin mice. The lack of an obvious peripheral neuropathy in these mice may reflect the fact that motor neurons in mice are much shorter than in humans, where their extreme length likely places more stringent requirements on the precise regulation of mitochondrial fusion. Although Mfn2-null animals die in utero, Mfn2^{R94Q} homozygous animals are born live and die at ~3 wk of age. The much milder phenotype of Mfn2^{R94Q} homozygous animals compared with Mfn2-null animals further supports our conclusion that Mfn2^{R94Q} can be partially complemented by endogenous Mfn1. Mfn2^{R94Q} homozygous animals have severe movement defects (unpublished data), and we are currently analyzing the basis for this phenotype.

In considering the effects of Mfn2 mutations, our results indicate that the full complement of mitofusins in any given cell

| A | Mitofusin complexes | | |
|-------------------------------|---------------------|-------------------------|--|
| | I | II | III |
| Wild-type cells | Mfn1/Mfn1 | Mfn1/Mfn2 | Mfn2/Mfn2 |
| B | CMT2A patients | | |
| most cells | Mfn1/Mfn1 | Mfn1/Mfn2 Mfn1/Mfn2* | Mfn2/Mfn2 Mfn2/Mfn2* Mfn2*/Mfn2* |
| cells with no Mfn1 expression | — | — | Mfn2/Mfn2 Mfn2/Mfn2* Mfn2*/Mfn2* |

Figure 8. Mfn1 complements mutant Mfn2 to preserve mitochondrial fusion in most CMT2A cells. (A) In most wild-type cell types, there are three classes of mitofusin complexes (I, II, and III) that maintain mitochondria in a highly dynamic state. (B) CMT2A patients are heterozygous for a mutant Mfn2 allele (designated Mfn2*). In most cells, defects in mitochondrial dynamics are mild because only a subset of class III complexes are nonfunctional (highlighted in black). In contrast, cells expressing little or no Mfn1 would suffer a large decline in mitochondrial fusion activity. Such cells contain only class III complexes, and the majority of these are nonfunctional.

type is the most relevant parameter in determining the dysfunction of mitochondrial fusion. This concept is clearly illustrated in our analysis of Mfn2 CMT2A mutations in MEFs. When Mfn2^{R94Q} is expressed in double Mfn-null cells, it is completely deficient for fusion activity, indicating that homooligomeric Mfn2^{R94Q} complexes are nonfunctional. In contrast, MEFs containing homozygous Mfn2^{R94Q} knockin mutations show only mild defects in mitochondrial morphology, a phenotype that is quite different from the extensive mitochondrial fragmentation observed in Mfn2-null MEFs. This observation indicates that in the presence of endogenous wild-type Mfn1, Mfn2^{R94Q} is actually highly functional. By expressing Mfn2^{R94Q} and other mutant alleles in Mfn1-null versus Mfn2-null cells, we found that wild-type Mfn1 but not Mfn2 can cooperate with mutant Mfn2 to promote mitochondrial fusion.

These results suggest that the widespread expression pattern of Mfn1 (Rojo et al., 2002; Santel et al., 2003) protects mitochondrial dynamics in most cells in CMT2A patients carrying nonfunctional alleles of Mfn2. CMT2A is an autosomal dominant disease, with patients carrying one mutant and one wild-type allele of Mfn2. In cell types that express Mfn1, Mfn1 homooligomeric complexes would be normal, and Mfn1–Mfn2 heterooligomeric complexes would also be largely normal as a result of the cooperation between Mfn1 and mutant Mfn2 (Fig. 8). For Mfn2 homooligomeric complexes, Mfn2^{wt}–Mfn2^{wt} complexes would be functional, whereas Mfn2^{wt}–Mfn2^{CMT2A} and Mfn2^{CMT2A}–Mfn2^{CMT2A} complexes would be nonfunctional. Therefore, of the three classes of mitofusin complexes, only a subset of one class is nonfunctional, resulting in mild mitochondrial fusion defects in most cells. In cell types with low or no Mfn1 expression, the full complement of mitofusin complexes consists primarily of Mfn2 homotypic complexes. In relative terms, such cells would experience a severe loss of mitochondrial fusion because the majority of mitofusin complexes (Mfn2^{wt}–Mfn2^{CMT2A} and Mfn2^{CMT2A}–Mfn2^{CMT2A}) lack mitochondrial fusion activity. Therefore, we propose that in CMT2A disease, the widespread expression pattern of Mfn1 serves to protect mitochondrial fusion in most cells through

heterooligomeric complex formation with mutant Mfn2. Peripheral nerves may contain little or no Mfn1 expression to compensate for mutant Mfn2. The resulting defects in mitochondrial dynamics coupled with the extreme length of these neurons lead to neuronal dysfunction and axon degeneration.

Our results emphasize the close interplay between Mfn1 and Mfn2 and the importance of the Mfn1–Mfn2 heterooligomeric complex in control of mitochondrial fusion. Finally, our results suggest that an important area of future study is the regulation of Mfn1 levels. Methods to increase Mfn1 expression in the peripheral nervous system may benefit CMT2A patients by promoting the complementation of mitochondrial fusion.

Materials and methods

Cloning and retroviral transduction

The mitofusin 7xMyc and 3xHA constructs were described previously (Chen et al., 2003). The CMT2A point mutations were introduced to Mfn2-7xMyc in pCDNA3.1 by PCR with primers encoding the mutations. After cloning, the entire amplified region was verified by sequencing. The mutant cDNAs were then cloned into the retroviral construct pCLBW, and viral supernatant was produced and collected as described previously (Chen et al., 2003).

Immunofluorescence

Immunofluorescence against Mfn2-7xMyc was performed as described previously (Chen et al., 2003). In brief, cells were grown on poly-L-lysine-treated coverslips, fixed in formalin, permeabilized with 0.1% Triton X-100 in PBS, and blocked with 5% bovine calf serum in PBS. The 9E10 primary antibody was detected with a Cy3-labeled secondary antibody. Coverslips were mounted with GelMount and imaged with a plan NeoFluar 63× NA 1.25 oil immersion objective (Carl Zeiss MicroImaging, Inc.) on a laser-scanning confocal microscope (model 410; Carl Zeiss MicroImaging, Inc.). Images were acquired with LSM software (version 1; Carl Zeiss MicroImaging, Inc.) and pseudocolored in Photoshop CS (Adobe). Mitochondria were visualized by mitochondrially targeted GFP or DsRed as previously described (Chen et al., 2005). In other cases, mitochondria were stained using 150 nM MitoTracker red CMXRos (Invitrogen) and post-fixed in acetone.

PEG fusion assay

PEG fusion assays were performed in the presence of cycloheximide as described previously (Chen et al., 2003, 2005). Cell hybrids were fixed 7 h after PEG treatment. The mitochondrial GFP signal was enhanced by incubation with an anti-GFP antibody conjugated to AlexaFluor488 (Invitrogen).

Derivation of Mfn2^{R94Q} homozygous MEFs

The two arms of the targeting construct were derived from Mfn2 genomic sequence (129/SvJ background) and subcloned into the targeting vector pPGKneobAlox2PGKDTA. Before subcloning of the left arm, the R94Q mutation was engineered into exon 5 by PCR. The targeting construct was verified by DNA sequencing. The linearized targeting construct was electroporated into low-passage 129/SvEv ES cells as described previously (Chen et al., 2003). Correctly targeted ES clones were identified by PCR using the primer sets A and B depicted in Fig. 3 A. Chimeric mice were generated by the injection of ES cells into C57BL/6 blastocysts. After confirmation of germline transmission, the floxed neomycin cassette was removed by mating the knockin mice with the EIIA-cre deleter line (Lakso et al., 1996). Heterozygous knockin animals were mated, and MEFs were derived from day 10.5 embryos as described previously (Chen et al., 2003). Homozygous embryos were identified by PCR genotyping of extra-embryonic membranes. Wild-type, Mfn1-null, Mfn2-null, and Mfn2^{R94Q}–Mfn2^{R94Q} MEFs were cultured in DME containing 10% bovine calf serum, 1 mM L-glutamine, and penicillin/streptomycin. Double Mfn-null MEFs were cultured with 10% FCS in place of bovine calf serum.

RNA isolation and RT-PCR

MEFs were resuspended directly in 800 μl STAT-60 (IsoTex Diagnostics, Inc.), and RNA was isolated according to the manufacturer's instructions. cDNA was generated by first-strand synthesis on total RNA using oligo(dT)

and Superscript II RT (Invitrogen). A cDNA fragment containing exon 5 was subsequently amplified (primers 5'-GGGGCCTACATCCAAGAGAG-3' and 5'-GCAGAACTTGTCCCAGAGC-3'). This product was digested overnight at 37°C with MspA11.

MEF lysates

MEF cell lysates were prepared from confluent 6-cm plates. For protein lysates, cells were washed once with PBS and resuspended in 400 μl lysis buffer (150 mM NaCl, 50 mM Tris, pH 8.0, 4 mM MgCl₂, 1% Triton X-100, and protease inhibitor cocktail [Roche]). Nuclei were removed by centrifugation, and postnuclear lysates were quantified with a protein assay (Bio-Rad Laboratories). 12 μg of each sample was separated by an 8% SDS-PAGE and immunoblotted with an anti-Mfn2 antibody (Sigma-Aldrich), an anti-Mfn1 antibody (Chen et al., 2003), or anti-β-actin as a loading control. Mitofusin antibodies (diluted 1:1,000) were detected by HRP-conjugated secondary antibodies and ECL detection reagents (GE Healthcare).

Coimmunoprecipitation assay

Double Mfn-null cells were infected with retrovirus encoding Mfn1-3xHA or Mfn2-3xHA. Infected cells were selected by culture in media containing bovine calf serum, which does not support uninfected double Mfn-null cells. Each cell line was subsequently infected with virus encoding Mfn2-7xMyc constructs or Drp1-7xMyc. Postnuclear lysates were generated as described above for MEFs (5–6 d after infection) and were immunoprecipitated with 9E10 antibody coupled to protein A–Sepharose beads. HA.11 (Covance) and 9E10 antibodies were used for immunoblotting.

Online supplemental material

Fig. S1 shows the mitochondrial profiles of MEFs expressing Mfn2 CMT2A alleles; this data is summarized in Fig. 1 C. Fig. S2 shows mitochondrial aggregation in MEFs highly overexpressing Mfn2 CMT2A alleles. Fig. S3 shows that at low infection rates, recombinant Mfn2 is present at approximately fourfold the level of endogenous Mfn2. Online supplemental material is available at <http://www.jcb.org/cgi/content/full/jcb.200611080/DC1>.

We are grateful to Hsiuchen Chen for helpful comments on the manuscript, members of the laboratory for encouragement, and the Beckman Imaging Center for use of confocal microscopes.

This work was supported by National Institutes of Health (NIH) grant GM062967. D.C. Chan was a Bren Scholar. S.A. Detmer was partially supported by NIH/National Research Service Award training grant 5T32GM07616.

Submitted: 15 November 2006

Accepted: 16 January 2007

References

- Alexander, C., M. Votruba, U.E. Pesch, D.L. Thiselton, S. Mayer, A. Moore, M. Rodriguez, U. Kellner, B. Leo-Kottler, G. Auburger, et al. 2000. OPA1, encoding a dynamin-related GTPase, is mutated in autosomal dominant optic atrophy linked to chromosome 3q28. *Nat. Genet.* 26:211–215.
- Chan, D.C. 2006. Mitochondrial fusion and fission in mammals. *Annu. Rev. Cell Dev. Biol.* 22:79–99.
- Chen, H., and D.C. Chan. 2006. Critical dependence of neurons on mitochondrial dynamics. *Curr. Opin. Cell Biol.* 18:453–459.
- Chen, H., S.A. Detmer, A.J. Ewald, E.E. Griffin, S.E. Fraser, and D.C. Chan. 2003. Mitofusins Mfn1 and Mfn2 coordinately regulate mitochondrial fusion and are essential for embryonic development. *J. Cell Biol.* 160:189–200.
- Chen, H., A. Chomyn, and D.C. Chan. 2005. Disruption of fusion results in mitochondrial heterogeneity and dysfunction. *J. Biol. Chem.* 280:26185–26192.
- Chung, K.W., S.B. Kim, K.D. Park, K.G. Choi, J.H. Lee, H.W. Eun, J.S. Suh, J.H. Hwang, W.K. Kim, B.C. Seo, et al. 2006. Early onset severe and late-onset mild Charcot-Marie-Tooth disease with mitofusin 2 (MFN2) mutations. *Brain.* 129:2103–2118.
- Cipolat, S., O. Martins de Brito, B. Dal Zilio, and L. Scorrano. 2004. OPA1 requires mitofusin 1 to promote mitochondrial fusion. *Proc. Natl. Acad. Sci. USA.* 101:15927–15932.
- Delettre, C., G. Lenaers, J.M. Griffioen, N. Gigarel, C. Lorenzo, P. Belenguer, L. Pelloquin, J. Grosgeorge, C. Turc-Carel, E. Perret, et al. 2000. Nuclear gene OPA1, encoding a mitochondrial dynamin-related protein, is mutated in dominant optic atrophy. *Nat. Genet.* 26:207–210.

- Eura, Y., N. Ishihara, S. Yokota, and K. Mihara. 2003. Two mitofusin proteins, mammalian homologues of FZO, with distinct functions are both required for mitochondrial fusion. *J. Biochem. (Tokyo)*. 134:333–344.
- Griffin, E.E., and D.C. Chan. 2006. Domain interactions within Fzo1 oligomers are essential for mitochondrial fusion. *J. Biol. Chem.* 281:16599–16606.
- Guo, X., G.T. Macleod, A. Wellington, F. Hu, S. Panchumarthi, M. Schoenfield, L. Marin, M.P. Charlton, H.L. Atwood, and K.E. Zinsmaier. 2005. The GTPase dMiro is required for axonal transport of mitochondria to *Drosophila* synapses. *Neuron*. 47:379–393.
- Ishihara, N., Y. Eura, and K. Mihara. 2004. Mitofusin 1 and 2 play distinct roles in mitochondrial fusion reactions via GTPase activity. *J. Cell Sci.* 117:6535–6546.
- Kijima, K., C. Numakura, H. Izumino, K. Umetsu, A. Nezu, T. Shiiki, M. Ogawa, Y. Ishizaki, T. Kitamura, Y. Shozawa, and K. Hayasaka. 2005. Mitochondrial GTPase mitofusin 2 mutation in Charcot-Marie-Tooth neuropathy type 2A. *Hum. Genet.* 116:23–27.
- Koshiba, T., S.A. Detmer, J.T. Kaiser, H. Chen, J.M. McCaffery, and D.C. Chan. 2004. Structural basis of mitochondrial tethering by mitofusin complexes. *Science*. 305:858–862.
- Lakso, M., J.G. Pichel, J.R. Gorman, B. Sauer, Y. Okamoto, E. Lee, F.W. Alt, and H. Westphal. 1996. Efficient in vivo manipulation of mouse genomic sequences at the zygote stage. *Proc. Natl. Acad. Sci. USA*. 93:5860–5865.
- Lawson, V.H., B.V. Graham, and K.M. Flanigan. 2005. Clinical and electrophysiologic features of CMT2A with mutations in the mitofusin 2 gene. *Neurology*. 65:197–204.
- Li, Z., K. Okamoto, Y. Hayashi, and M. Sheng. 2004. The importance of dendritic mitochondria in the morphogenesis and plasticity of spines and synapses. *Cell*. 119:873–887.
- Neuspiel, M., R. Zunino, S. Gangaraju, P. Rippstein, and H. McBride. 2005. Activated mitofusin 2 signals mitochondrial fusion, interferes with Bax activation, and reduces susceptibility to radical induced depolarization. *J. Biol. Chem.* 280:25060–25070.
- Okamoto, K., and J.M. Shaw. 2005. Mitochondrial morphology and dynamics in yeast and multicellular eukaryotes. *Annu. Rev. Genet.* 39:503–536.
- Olichon, A., L. Baricault, N. Gas, E. Guillou, A. Valette, P. Belenguer, and G. Lenaers. 2003. Loss of OPA1 perturbs the mitochondrial inner membrane structure and integrity, leading to cytochrome c release and apoptosis. *J. Biol. Chem.* 278:7743–7746.
- Rojo, M., F. Legros, D. Chateau, and A. Lombes. 2002. Membrane topology and mitochondrial targeting of mitofusins, ubiquitous mammalian homologs of the transmembrane GTPase Fzo. *J. Cell Sci.* 115:1663–1674.
- Santel, A., and M.T. Fuller. 2001. Control of mitochondrial morphology by a human mitofusin. *J. Cell Sci.* 114:867–874.
- Santel, A., S. Frank, B. Gaume, M. Herrler, R.J. Youle, and M.T. Fuller. 2003. Mitofusin-1 protein is a generally expressed mediator of mitochondrial fusion in mammalian cells. *J. Cell Sci.* 116:2763–2774.
- Stowers, R.S., L.J. Megeath, J. Gorska-Andrzejak, I.A. Meinertzhagen, and T.L. Schwarz. 2002. Axonal transport of mitochondria to synapses depends on Milton, a novel *Drosophila* protein. *Neuron*. 36:1063–1077.
- Sugioka, R., S. Shimizu, and Y. Tsujimoto. 2004. Fzo1, a protein involved in mitochondrial fusion, inhibits apoptosis. *J. Biol. Chem.* 279:52726–52734.
- Verhoeven, K., K.G. Claeys, S. Zuchner, J.M. Schroder, J. Weis, C. Ceuterick, A. Jordanova, E. Nelis, E. De Vriendt, M. Van Hul, et al. 2006. MFN2 mutation distribution and genotype/phenotype correlation in Charcot-Marie-Tooth type 2. *Brain*. 129:2093–2102.
- Verstreken, P., C.V. Ly, K.J. Venken, T.W. Koh, Y. Zhou, and H.J. Bellen. 2005. Synaptic mitochondria are critical for mobilization of reserve pool vesicles at *Drosophila* neuromuscular junctions. *Neuron*. 47:365–378.
- Youle, R.J., and M. Karbowski. 2005. Mitochondrial fission in apoptosis. *Nat. Rev. Mol. Cell Biol.* 6:657–663.
- Zuchner, S., and J.M. Vance. 2005. Emerging pathways for hereditary axonopathies. *J. Mol. Med.* 83:935–943.
- Zuchner, S., I.V. Mersiyanova, M. Muglia, N. Bissar-Tadmouri, J. Rochelle, E.L. Dadali, M. Zappia, E. Nelis, A. Patitucci, J. Senderek, et al. 2004. Mutations in the mitochondrial GTPase mitofusin 2 cause Charcot-Marie-Tooth neuropathy type 2A. *Nat. Genet.* 36:449–451.
- Zuchner, S., P. De Jonghe, A. Jordanova, K.G. Claeys, V. Guerguelcheva, S. Cherninkova, S.R. Hamilton, G. Van Stavern, K.M. Krajewski, J. Stajich, et al. 2006. Axonal neuropathy with optic atrophy is caused by mutations in mitofusin 2. *Ann. Neurol.* 59:276–281.